

Enhancing long-range order in disordered two-band s-wave superconductors

Heron Caldas,^{1,*} S. Rufo,^{2,3,†} and M. A. R. Griffith^{2,3,‡}

¹*Departamento de Ciências Naturais, Universidade Federal de São João Del Rei,
Praça Dom Helvécio 74, 36301-160, São João Del Rei, MG, Brazil*

²*Beijing Computational Science Research Center, Building 9, East Zone,
Nº 10 East Xibeiwang Road, Haidian District, Beijing 100193, China*

³*CeFEMA, Instituto Superior técnico, Universidade de Lisboa,
Av. Rovisco Pais, Nº 1, 1049-001 Lisboa, Portugal*

(Dated: March 20, 2023)

We investigate the effects of disorder in a hybridized two-dimensional two-band s-wave superconductor model. The situation in which electronic orbitals form these bands with angular momentum such that the hybridization $V_{i,j}$ among them is antisymmetric, under inversion symmetry, was taken into account. The on-site disorder is given by a random impurity potential W . We find that while the random disorder acts to the detriment of superconductivity, hybridization proceeds favoring it. Accordingly, hybridization plays an important role in two-band models of superconductivity, in order to hold the long-range order against the increase of disorder. This makes the present model eligible to describe real materials, since the hybridization may be induced by pressure or doping. In addition, the regime from moderate to strong disorder, reveals that the system is broken into superconductor islands with correlated local order parameters. These correlations persist to distances of several order lattice spacing which corresponds to the size of the SC-Islands.

I. INTRODUCTION

The experimental discovery of high transition temperature T_c in superconducting oxides [1] and the subsequent discoveries of strontium ruthenate [2], magnesium diboride [3], and iron pnictides [4, 5] have motivated an intense theoretical investigation in the superconducting properties of these materials. Several experiments have found that one of these compounds, magnesium diboride (MgB_2), with a transition temperature of ≈ 40 K [6], has two superconducting gaps [7–13] and, consequently, was classified as a two-band superconductor (SC) [14, 15].

Since in MgB_2 the relevant coupling mechanism is of intra-band character [16], two-band models have been employed to investigate materials possessing two pairing gaps. As pointed out in Ref. [17], the number of different gaps that emerge in multi-orbital systems is a direct consequence of the hybridization among the orbitals present in a given material. Actually, the Fermi surface (FS) of MgB_2 is determined by three orbitals, nevertheless, only two different BCS gaps are experimentally observed [18]. This happens because two of the three orbitals hybridize with each other forming one single band, responsible for a large superconducting σ band gap, while the non-hybridized orbital is related to the smaller superconducting at the π band gap.

It is worth mentioning that, besides inter-metallic binary superconductors such as MgB_2 , angle-resolved photoelectron spectroscopy (ARPES) experiments on La-based cuprates (with the hybridization of $d_{x^2-y^2}$ and d_{z^2}

orbitals) provides direct observation of a two-band structure [19]. In fact, there are several experiments with different materials, such as the Mo – Re binary solid solution alloys, that show evidence of multiband superconductivity [20, 21]. Supplementarily to these experimental investigations, two-band superconductors have been considered by various theoretical approaches as, for instance, in Refs. [22–24].

It is well known that disorder has tremendous consequences on conductors and superconductors. In a metal, the effect of disorder is to induce the Anderson localization of the electrons transforming a metal into an insulator, while in superconductors Cooper pair-localization results in superconductor-insulator transition (SIT). In a strong disorder regime, theoretical [26, 27] and experimental [28, 29] efforts show that the destruction of superconductivity and the SIT exhibit very unusual features. These intriguing features depend mostly on the path taken to reach the final state. For instance, it can assume, a metal, an insulator [27], a state without global superconductivity but with strong superconducting correlations [26] or a mixed state, composed of superconducting islands in an insulating sea; for a review, see Ref. [30]. Possible phase diagrams are further enriched when taking into account temperature effects, dimensionality, and the nature of the superconducting material, such as amorphous or granular thin films, nanowires, and crystalline superconductors [27, 30].

Thus, the effects of disorder in a superconductor bring about a competition of long-range phase coherence between electron pair states of the superconducting phase and the limitation of the spatial extent of the wave functions due to localization [31]. Then, it is natural to expect a critical disorder at which superconductivity is overcome. It was shown by Anderson [32] and Abrikosov and Gorkov (AG) [33] that nonmagnetic impurities have no

* hcaldas@ufsj.edu.br

† srufo@csrc.ac.cn

‡ griffithrufo@csrc.ac.cn

significant effect on the superconducting transition temperature in a zero magnetic field. However, as shown by Markowitz and Kadanoff [34], T_c is *de facto* suppressed due to gap anisotropy and impurity scattering. This suppression in a two-band model was shown later by Golubov and Mazin [35]. In this way, Anderson's and AG theories are applicable only to weakly disordered systems [36, 37]. In other words, the order parameter is insensitive to disorder (obeying Anderson's theorem) only in conventional superconductors [38], which means dilute disorder and spatially uniform order parameter. Experimentally, it has been observed that strong concentrations of nonmagnetic impurities, such as Zn, suppress the T_c [39–41].

Given the importance of MgB₂ superconductors due to their potential in a wide range of commercial applications [42–44], it becomes fundamental to know the effects of disorder on the physical properties of MgB₂ [45, 46]. Disorder has been introduced experimentally in MgB₂ by a series of distinct methods, and the suppression of T_c has been demonstrated by substitution (doping) experiments [47–58], neutron irradiation [59], and more recently by ion bombardment [60]. However, the complete (theoretical) understanding of the role of disorder in two-band superconductors is an open issue [61]. As pointed out in Ref. [62], the mechanism for disorder-induced T_c suppression in MgB₂ thin films has not been developed.

In this paper we investigate the effects of disorder in the superconducting properties of a simple two-band model, subjected to the hybridization of two single bands, namely a and b . We consider superconducting (s-wave) interactions only inside each band, which will result in intra-band pairing gaps Δ_a and Δ_b , respectively. The immediate consequence of hybridization is to transfer the quasiparticles among the bands and the clear advantage is that it can be adjusted experimentally by external factors like pressure or doping [65–67].

Using the Bogoliubov-de Gennes (BdG) mean-field theory we show the distribution of the local pairing amplitude $P(\Delta)$ and density of states $N(\omega)$ for various hybridization and disorder strengths. We analyze how a disorder modifies the behavior of the superconducting two-band model. We found that while the random disorder hinders superconductivity, hybridization favors it. Furthermore, for a strong disorder the system breaks into correlated islands in an insulating sea. This breaking is already known for a one-band system [63, 64]. The novelty here is the emergency of correlations between the a and b pairing regions, due to hybridization, and even the correlations between $a(b)$ and $a(b)$ pairing islands are hybridization dependent.

II. MODEL HAMILTONIAN

We study a generic two-band SC model in a two-dimensional (2D) Hubbard-type model, pictorially de-

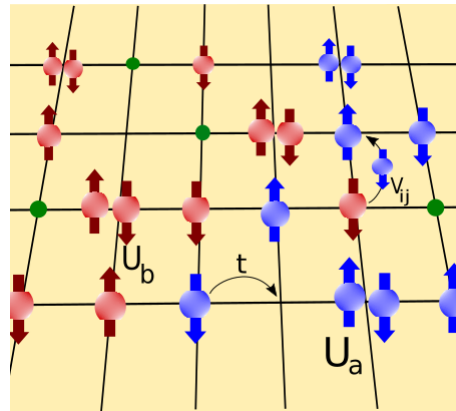


FIG. 1. (Color online) Schematic representation of the hybridized two-band attractive Hubbard model in the presence of disorder. Electrons from a (blue) and b (red)-bands can hop between lattice sites (lattice spacing a) with a hopping term t . The hybridization V_{ij} destroys an electron of band $a(b)$ and creates one in band $b(a)$ (without spin-flip), in a nearest neighbor site. Due to Pauli's principle, both hopping and hybridization are only possible if the final lattice site is empty or occupied with an electron with an opposite spin. The green spheres represent nonmagnetic impurities randomly distributed on the square lattice. Two electrons of band- $a(b)$ with opposite spin at the same site are subjected to an intra-band on-site interaction $U_{a(b)}$. For instance, consider the action of V_{ij} and the formation of a “blue pair” that will now experience the interaction potential U_a .

scribed in Fig. 1, and which Hamiltonian is given by

$$\begin{aligned}
 H = & - \sum_{\langle i,j \rangle, \sigma} t_{ij}^a a_{i,\sigma}^\dagger a_{j,\sigma} - \mu_a \sum_{i,\sigma} a_{i,\sigma}^\dagger a_{i,\sigma} \\
 & - \sum_{\langle i,j \rangle, \sigma} t_{ij}^b b_{i,\sigma}^\dagger b_{j,\sigma} - \mu_b \sum_{i,\sigma} b_{i,\sigma}^\dagger b_{i,\sigma} \\
 & + \sum_{\langle i,j \rangle, \sigma} V_{ij} (b_{i,\sigma}^\dagger a_{j,\sigma} + a_{i,\sigma}^\dagger b_{j,\sigma}) \\
 & - U_a \sum_i n_{i,\uparrow}^a n_{i,\downarrow}^a - U_b \sum_i n_{i,\uparrow}^b n_{i,\downarrow}^b, \quad (1)
 \end{aligned}$$

where $a_{i,\sigma}^\dagger$ ($a_{j,\sigma}$) and $b_{i,\sigma}^\dagger$ ($b_{j,\sigma}$) are the fermionic creation (annihilation) operator at site \mathbf{r}_i for the a and b bands, respectively, with spin $\sigma = \uparrow\downarrow$. The present square lattice has $a = 1$ (lattice spacing) and e chemical potentials $\mu_a = \mu + E_a$ and $\mu_b = \mu + E_b$. E_a and E_b are the bottoms of the a and b bands. $n_{i,\sigma}^a = a_{i,\sigma}^\dagger a_{i,\sigma}$ and $n_{i,\sigma}^b = b_{i,\sigma}^\dagger b_{i,\sigma}$ are the density operators, t_{ij}^a and t_{ij}^b are the hopping integrals between sites i and nearest neighbor j for each band. U_a (U_b) is the on-site attractive potential between the a (b) electrons. V_{ij} is the (k -dependent) nearest neighbors hybridization of the two bands, which may be symmetric or antisymmetric.

It has been shown that, in essence, all multiband superconductors have an odd-frequency (or equivalently odd-time) pairing component, which is induced in the bulk of the superconductor due to the breaking of the time

reverse, orbital, or spatial parity symmetry. Besides, the odd-frequency superconducting pairing requires only a finite band hybridization, and different intra-band order parameters (i.e., $\Delta_a \neq \Delta_b$), where only one of them needs to be superconducting [68]. So, here we consider a two-band model of a lattice of atoms with electronic orbitals of angular momentum l and $l + 1$. Due to the different parities of these orbital, the hybridization breaks inversion symmetry and is odd in k . Therefore, beyond the hopping of electrons in the same orbital, the hybridization between different orbitals in neighboring sites is also considered. Since these orbitals have angular momentum differing by an odd number, their wave-functions have opposite parities. Then, the hybridization between the orbitals in neighboring sites i and j is antisymmetric. Hence, we appraise an antisymmetric k -dependent hybridization $V(k)$ in Eq. (1) which in real space means $V_{ij} = -V_{ji}$. Another physical motivation for this choice is due to the fact that the antisymmetric hybridization which produces an odd-parity mixing between the a and b bands, is responsible for the p -wave nature of the induced inter-band pairing gap [69, 70]. As an example of the practical ‘‘utility’’ of p -wave gaps, we could mention 1D models with a pairing gap possessing p -wave symmetry, which is highly desirable for the investigation of the appearance of Majorana zero-energy bound states [71–74].

Notice that, in Hamiltonian Eq. (1) we have neglected the (rather involved) effects of Coulomb repulsion [64]. However, as will be clear below, even with such a simplification, the hybridized two-band model with attractive intra-band interactions and with disorder shows very interesting results which deserve to be investigated.

A. The Mean-Field Theory

The interaction part of the Hamiltonian in Eq. (1), with four fermionic operators, can be decoupled by the Hartree-Fock (HF) BCS decoupling (see appendix A) of two-body terms [75, 76], leading to the mean-field Hamiltonian (MFH) H_{MF} below

$$\begin{aligned}
H_{MF} = & - \sum_{\langle i,j \rangle, \sigma} t_{ij}^a a_{i\sigma}^\dagger a_{j\sigma} - \sum_{i, \sigma} (\tilde{\mu}_a - W_i) a_{i\sigma}^\dagger a_{i\sigma} \\
& - \sum_{\langle i,j \rangle, \sigma} t_{ij}^b b_{i\sigma}^\dagger b_{j\sigma} - \sum_{i, \sigma} (\tilde{\mu}_b - W_i) b_{i\sigma}^\dagger b_{i\sigma} \\
& - \sum_{\langle i,j \rangle, \sigma} V_{ij} (b_{i\sigma}^\dagger a_{j, \sigma} + a_{i\sigma}^\dagger b_{j, \sigma}) \\
& + \sum_i [\Delta_{a,i} a_{i, \uparrow}^\dagger a_{i, \downarrow}^\dagger + \Delta_{a,i}^* a_{i, \downarrow} a_{i, \uparrow}] \\
& + \sum_i [\Delta_{b,i} b_{i, \uparrow}^\dagger b_{i, \downarrow}^\dagger + \Delta_{b,i}^* b_{i, \downarrow} b_{i, \uparrow}], \quad (2)
\end{aligned}$$

where we have included the same local impurity potential W_i in both a and b bands, and $\tilde{\mu}_{p,i} = \mu_p + U_p < n_i^p > / 2$, where $p \equiv a, b$. Here $< n_i^p >$ is the average of the occu-

pation number. The strength of the disorder is defined by an independent random variable W_i uniformly distributed over $[-W, W]$, at each site \mathbf{r}_i . In this way, one can think of effective *local* chemical potentials given by $\mu_{p,i}^{eff} \equiv \tilde{\mu}_{p,i} - W_i$. This setup together with the intra-band interaction U_p and hybridization V_{ij} , are responsible for the rich physics and interesting phases scenario found here. For simplicity, but without loss of generality, we assume that $t_{ij}^a = t_{ij}^b = t$.

Then, the MFH in Eq. (2) describes a hybridized two-band s-wave superconductor, under the influence of random *nonmagnetic* impurities. In order to diagonalize H_{MF} for n^2 sites (n sites along $x(y)$ -direction), we firstly express Eq. (2) in matrix form $H_{MF} = \Psi^\dagger \mathcal{H} \Psi$, such that $\Psi^T = (a_{1\uparrow}^\dagger, \dots, a_{n^2\uparrow}^\dagger, b_{1\uparrow}^\dagger, \dots, b_{n^2\uparrow}^\dagger, a_{1\downarrow}, \dots, a_{n^2\downarrow}, b_{1\downarrow}, \dots, b_{n^2\downarrow})$. The MFH can be diagonalized by the transformation $M^\dagger \mathcal{H} M = \text{diag}(-E_1 \dots - E_{2N}; E_{2N} \dots E_1)$ for $N = n^2$, see appendix B.

The matrix elements of M can be related to coefficients of the Bogoliubov-Valatin transformation [77], defined in appendix B. Following this, the local particle densities and local pairing gaps can be expressed as

$$\langle n_i^a \rangle = 2 \sum_{n'=1}^N [|M_{i,2N+n'}|^2 f + |M_{i,3N+n'}|^2 (1-f)] \quad (3)$$

$$\langle n_i^b \rangle = 2 \sum_{n'=1}^N [|M_{i+N,2N+n'}|^2 f + |M_{i+N,3N+n'}|^2 (1-f)] \quad (4)$$

$$\Delta_{a,i} = U_a \sum_{n'=1}^N [M_{i,2N+n'} M_{i+2N,2N+n'} (1-2f)] \quad (5)$$

$$\Delta_{b,i} = U_b \sum_{n'=1}^N [M_{i+N,2N+n'} M_{i+3N,2N+n'} (1-2f)], \quad (6)$$

where $f \equiv f(E_{n'}) = 1/(e^{\beta E_{n'}} + 1)$, with $\beta = 1/k_B T$, is the Fermi function. The equations above form a system of $4N$ self-consistent equations. We numerically solved these equations for a lattice with $N = 144$ and $N = 400$ sites. The size of the matrix \mathcal{H} is $4N \times 4N$ and, therefore, needed a huge computational effort.

In the numerical calculations, we have used the antisymmetric property of the hybridization function i.e, $V_{ij} = -V_{ji}$, in order to ensure the odd-parity mixing between the a and b bands and to correctly describe the multiband superconductors [68], as discussed above. This choice is also appropriate for our model to describe, for example, the s and p -orbitals, which hybridize in different sub-lattices [78, 79].

More importantly, for the specific case of the MgB₂, it has been suggested from scanning tunneling spectroscopy (STS) vortex imaging that the superconductivity in the π -band is induced by the intrinsic superconductivity in the σ -band [80], by either inter-band scattering or Cooper pair tunneling [81]. In a recent paper [69], it has been demonstrated that the expressions

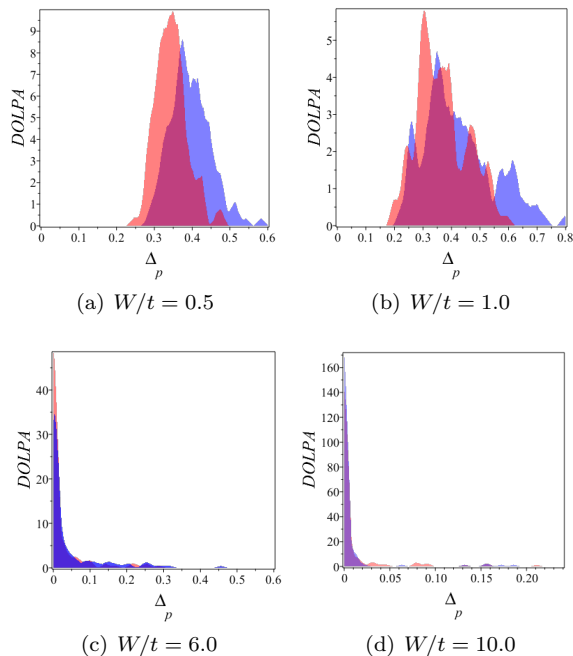


FIG. 2. (Color online) Distribution of the local pairing amplitudes DOLPA for a fixed hybridization $V/t = 0$ and various disorder strengths W/t and. We set $N = 144$, $U_a/t = 3.5$ and $U_b/t = 3$. The blue region stands for $p = a$, while the red one for $p = b$.

for the hybridization-induced pairing gap Δ_{ab} derived within a generic two-band superconductivity model (possessing pairing gaps Δ_a and Δ_b in a - and b -band, respectively), should obey: **i)** For a symmetric $V(k)$ the induced gap Δ_{ab} vanishes for Δ_a of the same order of magnitude as Δ_b , since $\Delta_{ab} \propto V(k)(\Delta_b - \Delta_a)$, as obtained previously in Ref. [68]. However, Δ_a approaches to Δ_b with the increasing of the nondimensional strength of the hybridization α , and equals to Δ_b even for relatively small α ($\alpha \lesssim 1$) [69]; **ii)** For an antisymmetric $V(k)$ the induced gap $\Delta_{ab} \propto V(k)\Delta_b + V(k)^*\Delta_a$, which means that Δ_{ab} will not vanish as Δ_a approaches to Δ_b . In truth, for an antisymmetric $V(k)$, Δ_a will eventually approach Δ_b , but only for $\alpha \gg 1$ ($\alpha \simeq 10$) [69]. These facts give us the confidence to adopt an antisymmetric hybridization $V(k)$ to model the two-band SC MgB₂ material.

III. RESULTS

The solutions of Eq. (3), (4), (5) and (6) provide N values for Δ_a , Δ_b , n_a and n_b . We defined a distribution of the local pairing amplitude (DOLPA), which tells us how homogeneous will be the order parameters Δ_p ($p = a, b$) in the whole lattice.

Physically, the dependence of the order parameters Δ_p on the hybridization can be understood by the following

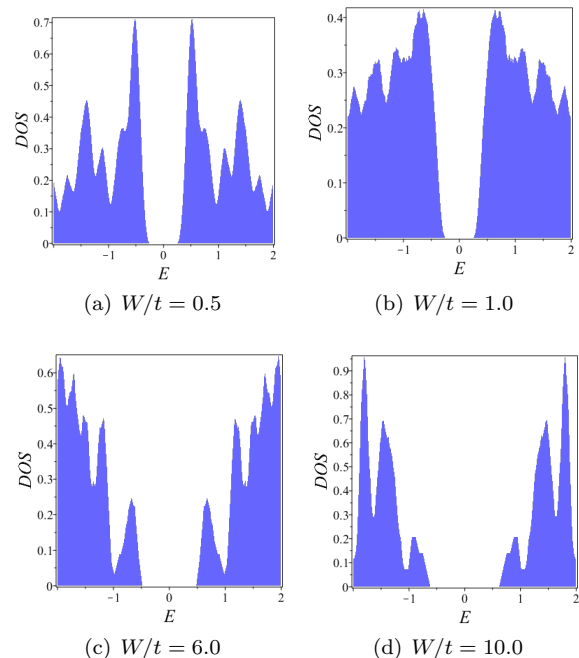


FIG. 3. (Color online) Density of states $N(\omega)$ for a fixed hybridization $V/t = 0$ and various disorder strengths W/t . We set $N = 144$, $U_a/t = 3.5$ and $U_b/t = 3$. Note that the spectral energy gap remains finite even at large W/t .

facts: The role of hybridization is to transfer the quasi-particles among the bands and this can be adjusted experimentally by external factors like pressure or doping. This process is formally equivalent to the one defined by a system polarized by an external magnetic field h with a Rashba spin-orbit (SOC) coupling between the spin-up and spin-down bands [85]. In this case, it has been found that the order parameter Δ is an increasing function of the SOC strength, since it enhances the density-of-states (DOS) $N(\varepsilon)$ at the Fermi surface [86, 87]. This equivalence can also be seen by examining the microscopic theory representing the system we just mentioned, in which the Rashba-type SOC term of the Hamiltonian describes the destruction of a fermion in one band and the creation of a fermion of opposite spin in the other band $H_{SOC} \propto a_{\mathbf{k}\downarrow}^\dagger b_{\mathbf{k}\uparrow}$, while the hybridization term is quite similar $H_{Hyb} \propto a_{\mathbf{k}\downarrow}^\dagger b_{\mathbf{k}\downarrow\uparrow}$. The $\downarrow\uparrow$ here means that the scattering processes described by the hybridization term can flip or maintain the same quasiparticle spin.

With this in mind, we proceed to investigate the systems in which both a - and b -bands have the same bare chemical potential namely, $\mu_a = \mu_b = \mu$ [88–90], and are affected by the same sort of (random) disorder in each site, that is $\mu_{a,i}^{eff} = \mu + U_a n_a / 2 - W_i$ and $\mu_{b,i}^{eff} = \mu + U_b n_b / 2 - W_i$, where $n^p = \langle n_i^p \rangle$, with $p = a, b$. For simplicity, we will make the approximation that the effective chemical potentials in both bands are given by a *shifted effective chemical potentials*, defined as

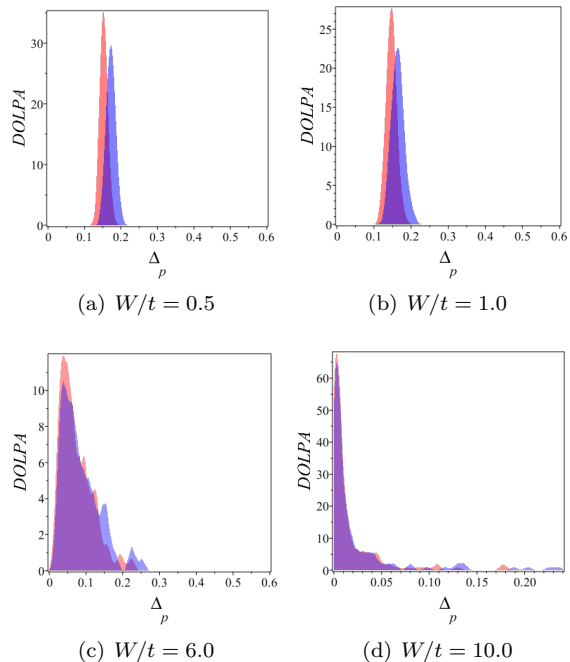


FIG. 4. (Color online) Distribution of the local pairing amplitudes DOLPA for a fixed hybridization $V/t = 2.0$ and various disorder strengths W/t and. We set $N = 144$, $U_a/t = 3.5$ and $U_b/t = 3$. The blue region stands for $p = a$, while the red one for $p = b$.

$\tilde{\mu}_{a,i}^{eff} = \mu_{a,i}^{eff} - U_a n^a / 2 = \mu - W_i = \tilde{\mu}_{b,i}^{eff}$. We have taken the strength of the attractive interaction $3 \leq U_{a,b}/t \leq 4$ since this is the range obtained in previous investigations of metal-to-insulator transition in disordered systems within the Hubbard model [83, 84].

In Fig. 2, we show the distribution of the local pairing amplitudes for a fixed hybridization $V/t = 0$ and various disorder strengths $W/t = 0.5, 1.0, 6.0$, and 10 . The blue and red regions are the distribution of the local pairing amplitude for Δ_a and Δ_b , respectively. Note that, as the disorder strength increases from Fig. 2 (a) to (d), the pairing amplitudes begin to concentrate around $\Delta_p = 0$, showing that strong disorder does not work to favor the superconducting state even in a two-band decoupled (i.e., $V/t = 0$) model. On the other hand, the density of states is presented in Fig. 3 for the same set of parameters in Fig. 2. Accordingly, we can observe the presence of a finite energy gap for each case. The same is observed for the one-band problem [64].

In order to verify the effect of a non-zero hybridization, we exhibit the distribution of the local pairing amplitudes and the density of states in Fig. 4 and Fig. 5, respectively.

For the same set of parameters in Fig. 2, but for a fixed hybridization $V/t = 2.0$, Fig. 4 shows the distribution of the local pairing amplitudes DOLPAR for various disorder strengths W . The blue and red regions also share the same meaning as Fig. 2. Accordingly, for low values of disorder, (a) $W/t = 0.5$ and (b) $W/t = 1.0$,

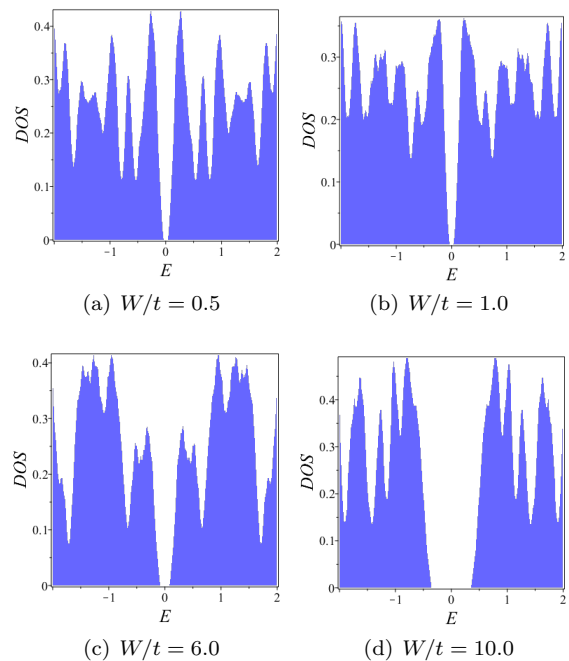


FIG. 5. (Color online) Density of states $N(\omega)$ for a fixed hybridization $V/t = 2.0$ and various disorder strengths W/t . We set $N = 144$, $U_a/t = 3.5$ and $U_b/t = 3$. Surprisingly, the increase of hybridization enhances the local superconducting order parameters making the whole system more robust against the disorder and the energy gap remains finite even at large W/t .

the pairing amplitudes begin to spread around the same value, approximately $\Delta_p = 0.15$. Interestingly, as the disorder increases, (c) $W/t = 6.0$ and (d) $W/t = 10.0$, both Δ_a and Δ_b remain spread at nonzero values. This means that the hybridization acts favoring superconductivity against disorder (see Fig. 2 (c) and (d) for $V/t = 0$, where the majority of Δ_p is around zero amplitude). This effect is expected for a certain range of the hybridization strength, where the antisymmetric hybridization increases the pairing gaps of a two-band model (without the disorder) [69, 82]. However, we found that even in the range of the hybridization that decreases the pairing gaps, the system is less sensitive against moderate disorder (i.e. for the same values of disorder in non-hybridized systems). We remark that the robustness of the hybridized two-band model against disorder can also be strengthened by the fact that the hybridization is responsible for correlations between pairs of different bands, and impurity scattering between them should be appropriately suppressed [91, 92]. Furthermore, the superconducting phase is sensitive to local perturbations in both orbitals. Since the hybridization acts connecting electrons from orbitals a and b , the correlations $\langle a_{\sigma,i}^\dagger b_{\sigma,i} \rangle$, $\langle a_{\uparrow,i} a_{\downarrow,i} \rangle$ and $\langle b_{\uparrow,i} b_{\downarrow,i} \rangle$ becomes strongly dependent on the hybridization.

After a numerical inspection in Fig. 3 and Fig. 5, one can verify that the hybridization V/t , disorder W/t , and

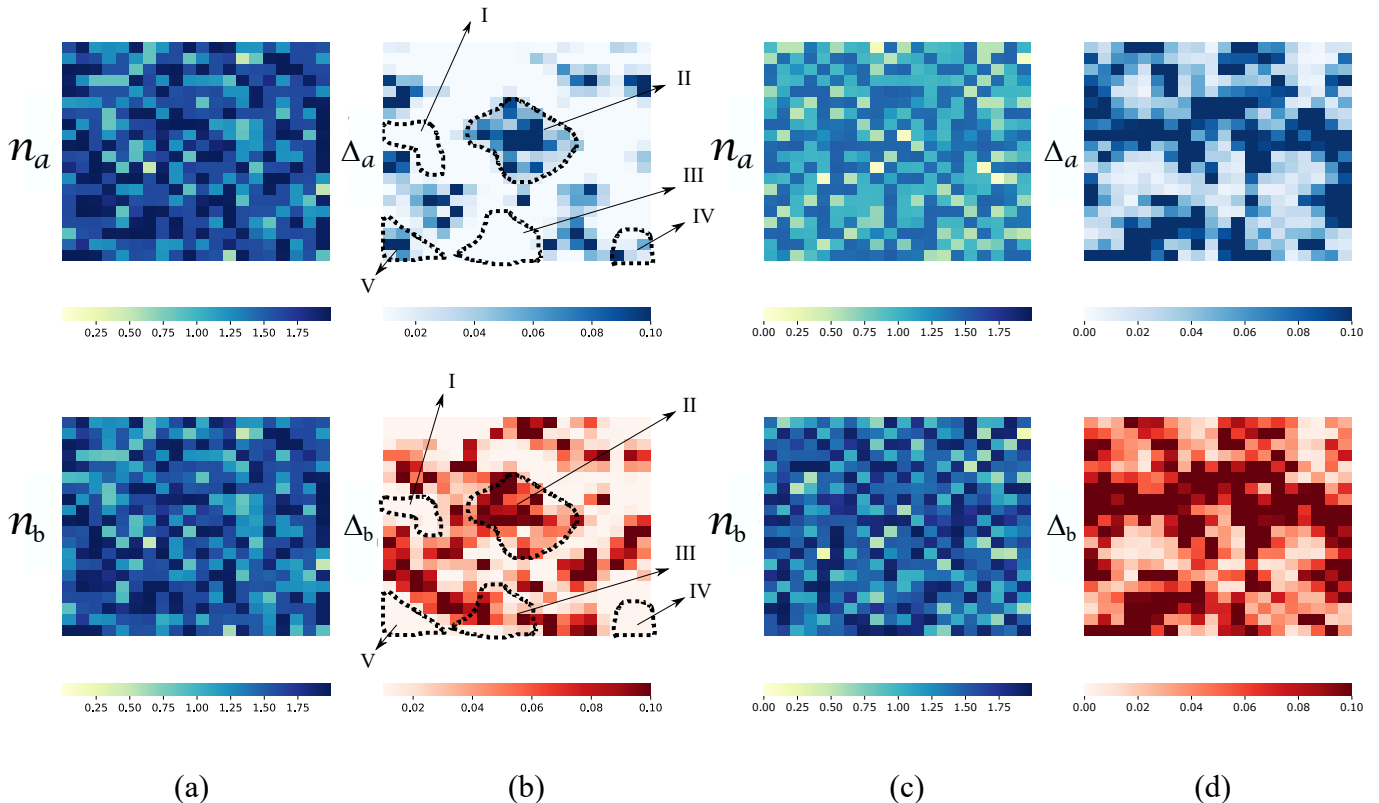


FIG. 6. (Color online) Local densities n_a and n_b ; local pairing amplitudes Δ_a and Δ_b as a function of hybridization, for a fixed $W/t = 6.0$, $\mu/t = 0.1$ and an ensemble of nine disorder realizations of 20×20 lattices. (a) Local densities and (b) Local pairing amplitudes for hybridization $V/t = 0.1$, where we highlight the regions I-Insulating ($\Delta_a = 0$ and $\Delta_b = 0$), II-mixed-superconducting ($\Delta_a \neq 0$ and $\Delta_b \neq 0$), III-superconducting type b ($\Delta_a = 0$ and $\Delta_b \neq 0$), IV and V-superconducting type a ($\Delta_a \neq 0$ and $\Delta_b = 0$). (c) Local densities and (d) Local pairing amplitudes for hybridization $V/t = 0.5$. Regions II, IV, and V denote the superconducting islands (SC-Islands). Note that the increase of the hybridization favors the II-mixed-superconducting region.

the gap energy ΔE possess a complex relationship. In particular, if $W/t = 0.5$, the energy gap is given by $\Delta_E = 0.298$ for $V/t = 0.0$, Fig. 3 (a), while it is greatly diminished to $\Delta_E = 0.16$ for $V/t = 2.0$, in Fig. 5 (a). By comparing these energy gap values, given the respective increasing values of V/t and fixed W/t , we can deduce that the hybridization, at least in the analyzed values, tends to result in a decreasing energy gap.

It is interesting to notice that the result of disorder in the density of states in Fig. 3 (c) and (d), shows the same effect displayed in Fig. 4 of the one-band model of Ref. [64], that also claims that while the disorder increases the singular pile-up at the gap edge smears out pushing states towards higher energies. However, the effect of the hybridization in Fig. 5 (c) and (d), is to “revert” the action of the disorder seen in Fig. 3 (c) and (d). In addition, Fig. 5 still presents a finite energy gap at large values of W/t . Attached to this result, we will present a discussion about the mitigation of the disorder

effect and enhancement of the long-range order against the increasing of the disorder, by calculating the pair-pair correlation, which is in agreement with the results of Fig. 4 and Fig. 5.

The results from Fig. 2 to Fig. 5, also show that no matter the regime of chemical potential and occupation number in the superconducting phase, the hybridized system tends to hold the long-range order against the increase of disorder.

To have a better understanding of the competition between the effects of disorder and hybridization in the whole system, we present in Fig. 6 a heatmap plot of the local densities n_a and n_b ; local pairing amplitudes Δ_a and Δ_b as a function of hybridization, for a fixed $W/t = 6.0$, $\mu/t = 0.1$ and an ensemble of nine disorder realizations of 20×20 lattices. (a) Local densities and (b) Local pairing amplitudes for hybridization $V/t = 0.1$. Looking for (b)(top and bottom), we highlight the regions I-Insulating ($\Delta_a = 0$ and $\Delta_b = 0$),

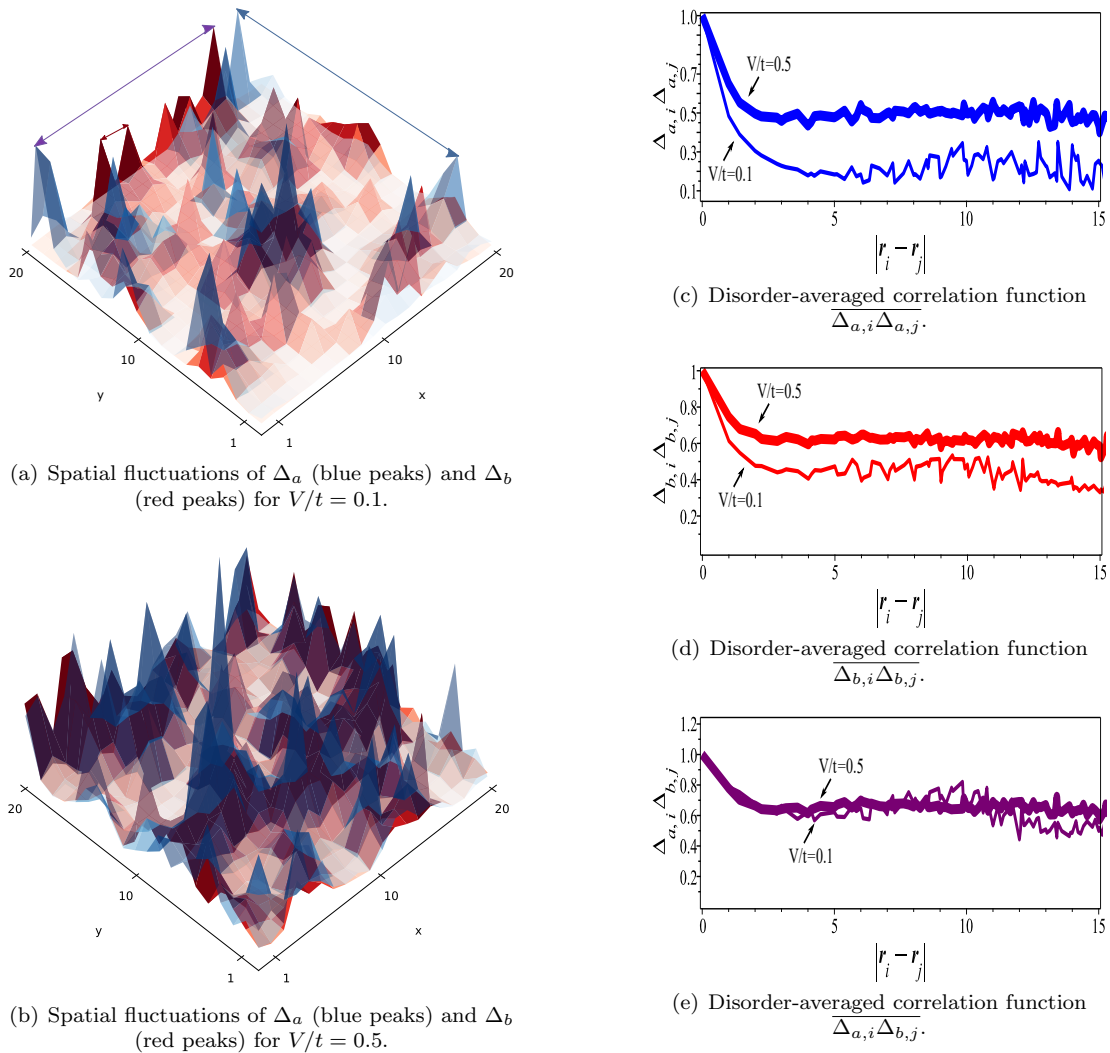


FIG. 7. (Color online). Spatial fluctuations of the local pairing amplitudes Δ_a and Δ_b in a 20×20 lattice, for $V/t = 0.1$ (a) and $V/t = 0.5$ (b). Following Fig. 6, we set $W/t = 6.0$ and $\mu/t = 0.1$. The blue arrows denote the coherent tunneling between $\Delta_{a,i}$ and $\Delta_{a,j}$ (blue peaks), the red arrows denote the coherent tunneling between $\Delta_{b,i}$ and $\Delta_{b,j}$ (red peaks) as well as the purple arrows denote the coherent tunneling between $\Delta_{a,i}$ and $\Delta_{b,j}$ (blue and red peaks). We present the disorder-averaged correlation function $\overline{\Delta_{a,i}\Delta_{a,j}}$ (c), $\overline{\Delta_{b,i}\Delta_{b,j}}$ (d) and $\overline{\Delta_{a,i}\Delta_{b,j}}$ (e). The thin curves are obtained for $V/t = 0.1$ while the thick one is for $V/t = 0.5$. Note that the correlations persist to distances of several order lattice spacing which corresponds to the SC-Islands size. We observe that the increasing of the hybridization tends to “suspend” and equalize the correlations $\overline{\Delta_{a,i}\Delta_{a,j}}$ and $\overline{\Delta_{b,i}\Delta_{b,j}}$. These results are normalized to be the unit for $|r_i - r_j| = 0$.

II-mixed-superconducting ($\Delta_a \neq 0$ and $\Delta_b \neq 0$), III-superconducting type b ($\Delta_a = 0$ and $\Delta_b \neq 0$), IV and V-superconducting type a ($\Delta_a \neq 0$ and $\Delta_b = 0$). (c) Local densities and (d) Local pairing amplitudes for hybridization $V/t = 0.5$. We then identify the presence of (local) superconducting islands (SC-Islands) in regions II, IV, and V, separated by an insulating one. We also observed that the presence of the SC-Islands is favored by the increase of U_a/t and W/t .

By comparing Fig. 6(b) and (d), we observe that the increase of the hybridization favors the II-mixed-superconducting region. For this reason, the spacial fluctuation of the lattice is modified. Revealing that the

coexistence of these complex structures has a highly non-homogenous formation.

Accordingly, as the disorder potential W/t is randomly assigned for each site we have uncorrelated local densities n_a and n_b , as we can see in Fig. 6 (a) and (c) with the absence of cluster formation [64]. Despite that, due to the self-consistent approach the local pairing amplitudes Δ_a and Δ_b present a spatial correlation between the SC-islands (regions II, III, IV and V in Fig. 6 (b)). This correlation occurs from moderate to high disorder values, in this case, $W/t = 6.0$. The typical size of a SC-Island is of the order of the coherence length ξ which is subjected to the disorder potential W/t , as well as, the effective

electron attraction U_a/t and U_b/t .

Thus, from Fig. 6 (b) and (d) we can see how the appearance of disorder implies a strong spatial fluctuation of the local order parameters Δ_p . To investigate this, in Fig. 7 (a) and (b) we show the spatial fluctuations for $V/t = 0.1$ and $V/t = 0.5$, respectively. The strong spatial fluctuation structure reveals where the order parameter gets a large amplitude, blue for Δ_a , red for Δ_b , and assuming a purple color where the SC-Island is in superposition. The correlation between the SC-Island is corroborated by the disorder-averaged correlation functions, $\overline{\Delta_{a,i}\Delta_{a,j}}$, $\overline{\Delta_{b,i}\Delta_{b,j}}$ and $\overline{\Delta_{a,i}\Delta_{b,j}}$, in Fig. 7 (c), (d) and (e), respectively. The average is performed for each set of $\Delta_{p,i}\Delta_{p',j}$ that share the same spatial distance $|r_i - r_j|$. The thin curves correspond to the correlation function for $V/t = 0.1$ while the thick curves for $V/t = 0.5$. The effect of increasing the hybridization make the correlations curves $\overline{\Delta_{a,i}\Delta_{a,j}}$, $\overline{\Delta_{b,i}\Delta_{b,j}}$ and $\overline{\Delta_{a,i}\Delta_{b,j}}$ to be much closer. Besides, the coherent tunneling of the Cooper pairs between the SC-Islands is the responsible for the establishment of correlation [93]. On the other hand, the regions with a relatively small Δ_p behave as an insulating phase with unpaired Cooper pair electrons. It is important to remark that we did not take into account quantum fluctuations in the phase ϕ of the order parameter (that would imply in gap parameters $\tilde{\Delta}_p = e^{i\phi}\Delta_p$), which are expected to destroy the long-range phase coherence between the small SC islands for strong disorder [64, 93].

A. Experimental Consequences

Let's discuss some experimental aspects of our two-band model subjected to disorder and hybridization. It is experimentally doable to grow homogeneously disordered films [94] that are disordered both on an atomic scale and granular films [95, 96]. These two types of films will essentially depend on the material, the substrate, and growth conditions [64]. For instance, a film of 99.99% Sn (or Pb) evaporated onto fire-polished glass substrates [95], or a 99.997% amorphous indium-oxide (In_2O_3) samples evaporated onto a SiO_2 substrate [97], where the effective disorder is controlled by the film thickness [94, 96]

In special, the maps in Fig. 6 could be useful as a guide to experimental measurements in order to identify regions with SC-Islands features. First, exposing a given superconducting material (that is well described as a two-band superconductor) to (random) disorder e.g., substitution, irradiation, growing, etc, and then measuring it with a scanning tunneling microscopy (STM) probe, should be feasible to verify that the DOS is distributed in a wide energy range, with more states in higher energies, as in Fig. 3. So, by turning on the hybridization, the STM measurements should now find a concentration in the DOS near the gap edges, as in Fig. 5.

In contrast with the one-band model studied in Ref. [64], we remark that the mixed-superconducting

phase appeared only in the context of the highly hybridized two-band model, as explored here. We also expect that landscapes showing the regions with insulating, superconducting, and mixed-SC-Islands should be visible through STM, as the topography images of a ' π' -shaped Pb island sitting on top of a striped incommensurate (SIC) surface [98].

IV. CONCLUSION

Here, we investigated the effects of disorder in the superconducting properties of a simple hybridized two-band model. Motivated by the superconductor MgB_2 , we look for both disorder and an antisymmetric hybridization in the cases where there are s-wave intra-band interactions only inside each of the two bands. The impurity potential is given by an independent random variable W which controls the strength of the disorder. Experimentally, the disorder can be controlled by varying the film thickness. On the other hand, the hybridization between the two bands can be tunable by applying strain or by carrier doping. We found that while (the random disorder) W acts to the detriment of the superconductivity (driving to zero the pairing gap parameter through suppression of the superconducting phase in favor of an insulating one), hybridization makes the system more robust against disorder effects.

We also found that strong disorder implies in a prominent spatial fluctuation of the local order parameters Δ_a and Δ_b , which are correlated. These correlations persevere to distances of several order lattice spacing which corresponds to the size of the SC-Islands.

For future investigation, we propose to look for the 2D version of the present two-band hybridized system, also in the presence of disorder and under a static magnetic field h parallel to the 2D plane [99]. Given the variety of external effects, hybridization V , disorder W , and magnetic field h , we hope for the emergence of new and possibly exotic phases.

V. ACKNOWLEDGMENTS

We thank D. Nozadze and N. Trivedi for enlightening discussions. We wish to thank CAPES and CNPq, Brazil agencies, as well as, the Beijing Computational Science Research Center-CSRC in China, and CeFEMA-IST in Portugal for partial financial support.

Appendix A: Mean Field Decoupling for interaction terms

where $\psi_{\uparrow,\downarrow} = a_{\uparrow,\downarrow}, b_{\uparrow,\downarrow}$. The ‘‘Fock condensates’’ are zero here, so $\langle \psi_{\uparrow}^{\dagger} \psi_{\downarrow} \rangle = \langle \psi_{\downarrow}^{\dagger} \psi_{\uparrow} \rangle = 0$ in Eqs. (A2, A3 and A4 below and consequently in Eq. (2).

$$\begin{aligned} \psi_{\uparrow}^{\dagger} \psi_{\downarrow}^{\dagger} \psi_{\downarrow} \psi_{\uparrow} &= \tag{A1} \\ &\langle \psi_{\downarrow} \psi_{\uparrow} \rangle \psi_{\uparrow}^{\dagger} \psi_{\downarrow}^{\dagger} + \langle \psi_{\uparrow}^{\dagger} \psi_{\downarrow}^{\dagger} \rangle \psi_{\downarrow} \psi_{\uparrow} - |\langle \psi_{\downarrow} \psi_{\uparrow} \rangle|^2 \\ &+ \langle \psi_{\uparrow}^{\dagger} \psi_{\uparrow} \rangle \psi_{\downarrow}^{\dagger} \psi_{\downarrow} + \langle \psi_{\downarrow}^{\dagger} \psi_{\downarrow} \rangle \psi_{\uparrow}^{\dagger} \psi_{\uparrow} - \langle \psi_{\uparrow}^{\dagger} \psi_{\uparrow} \rangle \langle \psi_{\downarrow}^{\dagger} \psi_{\downarrow} \rangle \\ &- (\langle \psi_{\uparrow}^{\dagger} \psi_{\downarrow} \rangle \psi_{\downarrow}^{\dagger} \psi_{\uparrow} + \langle \psi_{\downarrow}^{\dagger} \psi_{\uparrow} \rangle \psi_{\uparrow}^{\dagger} \psi_{\downarrow}), \end{aligned}$$

$$\begin{aligned} -U_a \sum_i a_{i,\uparrow}^{\dagger} a_{i,\downarrow}^{\dagger} a_{i,\downarrow} a_{i,\uparrow} &= -U_a \sum_i [\langle a_{i,\downarrow} a_{i,\uparrow} \rangle a_{i,\uparrow}^{\dagger} a_{i,\downarrow}^{\dagger} + \langle a_{i,\uparrow}^{\dagger} a_{i,\downarrow}^{\dagger} \rangle a_{i,\downarrow} a_{i,\uparrow} - |\langle a_{i,\downarrow} a_{i,\uparrow} \rangle|^2 \tag{A2} \\ &+ \langle a_{i,\uparrow}^{\dagger} a_{i,\uparrow} \rangle a_{i,\downarrow}^{\dagger} a_{i,\downarrow} + \langle a_{i,\downarrow}^{\dagger} a_{i,\downarrow} \rangle a_{i,\uparrow}^{\dagger} a_{i,\uparrow} - \langle a_{i,\uparrow}^{\dagger} a_{i,\uparrow} \rangle \langle a_{i,\downarrow}^{\dagger} a_{i,\downarrow} \rangle], \end{aligned}$$

$$\begin{aligned} -U_b \sum_i b_{i,\uparrow}^{\dagger} b_{i,\downarrow}^{\dagger} b_{i,\downarrow} b_{i,\uparrow} &= -U_b \sum_i [\langle b_{i,\downarrow} b_{i,\uparrow} \rangle b_{i,\uparrow}^{\dagger} b_{i,\downarrow}^{\dagger} + \langle b_{i,\uparrow}^{\dagger} b_{i,\downarrow}^{\dagger} \rangle b_{i,\downarrow} b_{i,\uparrow} - |\langle b_{i,\downarrow} b_{i,\uparrow} \rangle|^2 \tag{A3} \\ &+ \langle b_{i,\uparrow}^{\dagger} b_{i,\uparrow} \rangle b_{i,\downarrow}^{\dagger} b_{i,\downarrow} + \langle b_{i,\downarrow}^{\dagger} b_{i,\downarrow} \rangle b_{i,\uparrow}^{\dagger} b_{i,\uparrow} - \langle b_{i,\uparrow}^{\dagger} b_{i,\uparrow} \rangle \langle b_{i,\downarrow}^{\dagger} b_{i,\downarrow} \rangle]. \end{aligned}$$

Defining $\Delta_{a,i} = -U_a \langle a_{i,\downarrow} a_{i,\uparrow} \rangle$, $\Delta_{b,i} = -U_b \langle b_{i,\downarrow} b_{i,\uparrow} \rangle$, $\langle n_{i,\sigma}^a \rangle = \langle a_{i,\sigma}^{\dagger} a_{i,\sigma} \rangle$ and $\langle n_{i,\sigma}^b \rangle = \langle b_{i,\sigma}^{\dagger} b_{i,\sigma} \rangle$, the interaction term reduces to

$$\begin{aligned} H_{int} &= \sum_i \Delta_{a,i} a_{i,\uparrow}^{\dagger} a_{i,\downarrow}^{\dagger} + \Delta_{a,i}^* a_{i,\downarrow} a_{i,\uparrow} + |\Delta_{a,i}|^2 / U_a - U_a [\langle n_{i,\uparrow}^a \rangle a_{i,\downarrow}^{\dagger} a_{i,\downarrow} + \langle n_{i,\downarrow}^a \rangle a_{i,\uparrow}^{\dagger} a_{i,\uparrow} - \langle n_{i,\uparrow}^a \rangle \langle n_{i,\downarrow}^a \rangle] \\ &+ \sum_i \Delta_{b,i} b_{i,\uparrow}^{\dagger} b_{i,\downarrow}^{\dagger} + \Delta_{b,i}^* b_{i,\downarrow} b_{i,\uparrow} + |\Delta_{b,i}|^2 / U_b - U_b [\langle n_{i,\uparrow}^b \rangle a_{i,\downarrow}^{\dagger} b_{i,\downarrow} + \langle n_{i,\downarrow}^b \rangle b_{i,\uparrow}^{\dagger} b_{i,\uparrow} - \langle n_{i,\uparrow}^b \rangle \langle n_{i,\downarrow}^b \rangle]. \tag{A4} \end{aligned}$$

Appendix B: Hamiltonian in real space

Defining the base $\Psi^T = (a_{1\uparrow}^{\dagger}, \dots, a_{n^2\uparrow}^{\dagger}, b_{1\uparrow}^{\dagger}, \dots, b_{n^2\uparrow}^{\dagger}, a_{1\downarrow}, \dots, a_{n^2\downarrow}, b_{1\downarrow}, \dots, b_{n^2\downarrow})$, we can write HMF as $H_{MF} = \Psi^{\dagger} \mathcal{H} \Psi$, where $\mathcal{H} = \mathcal{H}_{4N \times 4N}$ for $N = n^2$. The Matrix \mathcal{H} is given by

$$\mathcal{H} = \begin{pmatrix} A & V & \Delta_{aa} & 0 \\ V & B & 0 & \Delta_{bb} \\ \Delta_{aa} & 0 & -A & -V \\ 0 & \Delta_{bb} & -V & -B \end{pmatrix}, \tag{B1}$$

where $A, V, B, \Delta_{\eta\eta}$ are matrices $N \times N$. Here, A is formed by on-site energy and hopping terms between electrons of the orbital a . The matrix B is formed by on-site energy and hopping terms between electrons of the orbital b . The matrix V is the subspace of the hybridization and $\Delta_{aa,bb}$ are formed by superconducting order parameters from orbitals a and b , respectively.

In order to diagonalize H_{MF} , we defined a matrix M . The matrix M acts in the basis Ψ as

$$\Psi = M \Phi \tag{B2}$$

or, explicitly

$$\begin{pmatrix} a_{\uparrow 1} \\ \vdots \\ a_{\uparrow N} \\ b_{\uparrow 1} \\ \vdots \\ b_{\uparrow N} \\ a_{\downarrow 1}^\dagger \\ \vdots \\ a_{\downarrow N}^\dagger \\ b_{\downarrow 1}^\dagger \\ \vdots \\ b_{\downarrow N}^\dagger \end{pmatrix} = \begin{pmatrix} M_{1,1} & \cdots & M_{1,N} & M_{1,N+1} & \cdots & M_{1,2N} & M_{1,2N+1} & \cdots & M_{1,3N} & M_{1,3N+1} & \cdots & M_{1,4N} \\ \vdots & \vdots & \vdots & \ddots & \vdots \\ M_{N,1} & \cdots & M_{N,N} & M_{N,N+1} & \cdots & M_{N,2N} & M_{N,2N+1} & \cdots & M_{N,3N} & M_{N,3N+1} & \cdots & M_{N,4N} \\ M_{N+1,1} & \cdots & M_{N+1,N} & M_{N+1,N+1} & \cdots & M_{N+1,2N} & M_{N+1,2N+1} & \cdots & M_{N+1,3N} & M_{N+1,3N+1} & \cdots & M_{N+1,4N} \\ \vdots & \vdots & \vdots & \ddots & \vdots \\ M_{2N,1} & \cdots & M_{2N,N} & M_{2N,N+1} & \cdots & M_{2N,2N} & M_{2N,2N+1} & \cdots & M_{2N,3N} & M_{2N,3N+1} & \cdots & M_{2N,4N} \\ M_{2N+1,1} & \cdots & M_{2N+1,N} & M_{2N+1,N+1} & \cdots & M_{2N+1,2N} & M_{2N+1,2N+1} & \cdots & M_{2N+1,3N} & M_{2N+1,3N+1} & \cdots & M_{2N+1,4N} \\ \vdots & \vdots & \vdots & \ddots & \vdots \\ M_{3N,1} & \cdots & M_{3N,N} & M_{3N,N+1} & \cdots & M_{3N,2N} & M_{3N,2N+1} & \cdots & M_{3N,3N} & M_{3N,3N+1} & \cdots & M_{3N,4N} \\ M_{3N+1,1} & \cdots & M_{3N+1,N} & M_{3N+1,N+1} & \cdots & M_{3N+1,2N} & M_{3N+1,2N+1} & \cdots & M_{3N+1,3N} & M_{3N+1,3N+1} & \cdots & M_{3N+1,4N} \\ \vdots & \vdots & \vdots & \ddots & \vdots \\ M_{4N,1} & \cdots & M_{4N,N} & M_{4N,N+1} & \cdots & M_{4N,2N} & M_{4N,2N+1} & \cdots & M_{4N,3N} & M_{4N,3N+1} & \cdots & M_{4N,4N} \end{pmatrix} \begin{pmatrix} \alpha_{\uparrow 1} \\ \vdots \\ \alpha_{\uparrow N} \\ \alpha_{\uparrow 1} \\ \vdots \\ \alpha_{\uparrow N} \\ \alpha_{\downarrow 1}^\dagger \\ \vdots \\ \alpha_{\downarrow N}^\dagger \\ \alpha_{\downarrow 1}^\dagger \\ \vdots \\ \alpha_{\downarrow N}^\dagger \end{pmatrix} \quad (\text{B3})$$

such that, the new base $\Phi^T = (\alpha_{1\uparrow}^\dagger, \dots, \alpha_{N\uparrow}^\dagger, \alpha_{1\uparrow}, \dots, \alpha_{N\uparrow}, \alpha_{1\downarrow}, \dots, \alpha_{N\downarrow}, \alpha_{1\downarrow}^\dagger, \dots, \alpha_{N\downarrow}^\dagger)$ is a base where H_{MF} become diagonal

$$M^\dagger H_{MF} M = \text{diag}(-E_1 \dots - E_{2N}; E_{2N} \dots E_1) \quad (\text{B4})$$

We call attention to fact that the columns of M are the eigenvectors of H_{MF} . We organized the eigenvalues of H_{MF} from the lesser to greater values (i. e. $-E_1 \dots - E_{2N}, E_{2N} \dots E_1$) and therefore, note that, the last $2N$ columns of M contain all eigenvectors that are related to positive energies of the Hamiltonian H_{MF} .

The Bogoliubov-Valatin transformations can be defined according the Eq. B3 in the following way

$$a_{i,\uparrow} = \sum_{n'=1}^N [M_{i,2N+n'} \alpha_{2N+n',\uparrow} - M_{i,3N+n'} \alpha_{3N+n',\downarrow}^\dagger], \quad (\text{B5})$$

$$b_{i,\uparrow} = \sum_{n'=1}^N [M_{i+N,2N+n'} \alpha_{2N+n',\uparrow} - M_{i+N,3N+n'} \alpha_{3N+n',\downarrow}^\dagger], \quad (\text{B6})$$

$$a_{i,\downarrow} = \sum_{n'=1}^N [M_{i+2N,2N+n'} \alpha_{2N+n',\uparrow} + M_{i+2N,3N+n'}^* \alpha_{3N+n',\downarrow}^\dagger], \quad (\text{B7})$$

$$b_{i,\downarrow} = \sum_{n'=1}^{N^2} [M_{i+3N,2N+n'} \alpha_{2N+n',\uparrow} + M_{i+3N,3N+n'}^* \alpha_{3N+n',\downarrow}^\dagger], \quad (\text{B8})$$

where the sum only runs over n' corresponding to positive eigenvalues. The Eqs. B5-B8 are nothing more than the product of a line of M by the vector Φ .

-
- [1] J. G. Bednorz and K. A. Müller, Z. Phys. B: Condens. Matter **64**, 189 (1986); K. A. Müller and J. G. Bednorz, Science **237**, 1133 (1987).
- [2] Y. Maeno, H. Hashimoto, K. Yoshida, S. Nishizaki, T. Fujita, J. G. Bednorz, and F. Lichtenberg, Nature London **372**, 532 (1994).
- [3] J. Nagamatsu, N. Nakagawa, T. Muranaka, Y. Zenitani, and J. Akimitsu, Nature London **410**, **63** (2001).
- [4] Y. Kamihara, H. Hiramatsu, M. Hirano, R. Kawamura, H. Yanagi, T. Kamiya, and H. Hosono, J. Am. Chem. Soc. **128**, 10012 (2006).
- [5] Y. Kamihara, T. Watanabe, M. Hirano, and H. Hosono, J. Am. Chem. Soc. **130**, 3296 (2008).
- [6] J. Nagamatsu, N. Nakagawa, T. Muranaka, Y. Zenitani, and J. Akimitsu, Nature London **410**, 41 (2001).
- [7] Y. Wang, T. Plackowski, A. Junod, Physica C **355**, 179 (2001).
- [8] F. Bouquet, R. A. Fisher, N. E. Phillips, D. G. Hinks, and J. D. Jorgensen, Phys. Rev. Lett. **87**, 047001 (2001).
- [9] H. D. Yang, J.-Y. Lin, H. H. Li, F. H. Hsu, C. J. Liu,

- S.-C. Li, R.-C. Yu, and C.-Q. Jin, *Phys. Rev. Lett.* **87**, 167003 (2001).
- [10] P. Szabó, P. Samuely, J. Kačmarčík, T. Klein, J. Marcus, D. Fruchart, S. Miraglia, C. Marcenat, and A. G. M. Jansen, *Phys. Rev. Lett.* **87**, 137005 (2001).
- [11] F. Giubileo, D. Roditchev, W. Sacks, R. Lamy, D. X. Thanh, J. Klein, S. Miraglia, D. Fruchart, J. Marcus, and Ph. Monod, *Phys. Rev. Lett.* **87**, 177008 (2001).
- [12] X. K. Chen, M. J. Konstantinović, J. C. Irwin, D. D. Lawrie, and J. P. Franck, *Phys. Rev. Lett.* **87**, 157002 (2001).
- [13] S. Tsuda, T. Yokoya, T. Kiss, Y. Takano, K. Togano, H. Kito, H. Ihara, and S. Shin, *Phys. Rev. Lett.* **87**, 177006 (2001).
- [14] S. Souma, Y. Machida, T. Sato, et al., *Nature* **423**, 65 (2003).
- [15] J. Geerk, R. Schneider, G. Linker, A. G. Zaitsev, R. Heid, K.-P. Bohnen, and H. v. Löhneysen, *Phys. Rev. Lett.* **94**, 227005 (2005).
- [16] A. Y. Liu, I. I. Mazin, and J. Kortus, *Phys. Rev. Lett.* **87**, 087005 (2001).
- [17] A. Moreo, M. Daghofer, J. A. Riera, and E. Dagotto, *Phys. Rev. B* **79**, 134502 (2009).
- [18] H. J. Choi, D. Roundy, H. Sun, M. L. Cohen, and S. G. Louie, *Nature London* **418**, 758 (2002).
- [19] C. E. Matt, D. Sutter, A. M. Cook, Y. Sassa, M. Mansson, O. Tjernberg, L. Das, M. Horio, D. Destraz, C. G. Fatuzzo, et al., *Nature Comm.* **9**, 972 (2018).
- [20] S. Sundar, L. S. S. Chandra, M. K. Chattopadhyay, and S. B. Roy, *J. Phys.: Condens. Matter* **27**, 045701 (2015).
- [21] S. Sundar, L. S. S. Chandra, M. K. Chattopadhyay, S. K. Pandey, D. Venkateshwarlu, R. Rawat, V. Ganesan, and S. B. Roy, *New J. Phys.* **17**, 053003 (2015).
- [22] Y. S. Yerin and A. N. Omelyanchouk, *Low Temp. Phys.* **33**, 401 (2007).
- [23] Y. S. Erin, S. V. Kuplevakhskii, and A. N. Omel'yanchuk, *Low Temp. Phys.* **34**, 891 (2008).
- [24] D. V. Efremov, M. M. Korshunov, O. V. Dolgov, A. A. Golubov, and P. J. Hirschfeld, *Phys. Rev. B* **84**, 180512(R) (2011).
- [25] A. M. Finkel'stein, *Pis'ma Zh. Eksp. Teor. Fiz.* **45**, 37 (1987) [*Sov. Phys. JETP Lett.* **45**, 46 (1987)].
- [26] M. V. Feigel'man, L. B. Ioffe, V. E. Kravtsov, and E. A. Yuzbashyan, *Phys. Rev. Lett.* **98**, 027001 (2007); *Ann. Phys. (N.Y.)* **325**, 1390 (2010).
- [27] B. Sacépé, M. Feigel'man and T. M. Klapwijk, *Nature Phys.* **16**, 734 (2020).
- [28] B. Sacépé, T. Dubouchet, C. Chapelier, et al., *Nature Phys.* **7**, 239 (2011).
- [29] M. Mondal, A. Kamlapure, M. Chand, G. Saraswat, S. Kumar, J. Jesudasan, L. Benfatto, V. Tripathi, and P. Raychaudhuri, *Phys. Rev. Lett.* **106**, 047001 (2011).
- [30] V. Dobrosavljevic, N. Trivedi, and J. M. Valles Jr., *Conductor Insulator Quantum Phase Transitions*. Part II. (Oxford University Press, 2012).
- [31] A. M. Goldman and N. Marković, *Phys. Today* **51** (11), 39 (1998).
- [32] P. W. Anderson, *J. Phys. Chem. Solids* **11**, 26 (1959).
- [33] A. A. Abrikosov and L. P. Gorkov, *Zh. Éksp. Teor. Fiz.* **36**, 319 (1959) [*Sov. Phys. JETP* **9**, 220 (1959)].
- [34] D. Markowitz and L.P. Kadanoff, *Phys. Rev.* **131**, 563 (1963).
- [35] A. A. Golubov, and I. I. Mazin, *Phys. Rev. B* **55**, 15146 (1997).
- [36] D. Belitz and T. Kirkpatrick, *Rev. Mod. Phys.* **66**, 261 (1994).
- [37] R. Moradian and H. Mousavi, *J. Phys.: Condens. Matter* **20**, 095212 (2008).
- [38] M. N. Gastiasoro and B. M. Andersen, *Phys. Rev. B* **98**, 184510 (2018).
- [39] H. Alloul, J. Bobroff, M. Gabay, and P. J. Hirschfeld, *Rev. Mod. Phys.* **81**, 45 (2009).
- [40] J. Li et al., *Phys. Rev. B* **85**, 214509 (2012).
- [41] J. Li et al., *Nature Comm.* **6**, 7614 (2015).
- [42] J. Rowell, *Nature Mater* **1**, 5 (2002).
- [43] T. Tan, M. A. Wolak, X. X. Xi, T. Tajima, and L. Civale, *Sci. Rep.* **6** 35879, (2016).
- [44] W. N. Kang, H.-J. Kim, E.-M. Choi, C. U. Jung, and S.-I. Lee, *Science*, **292** 1521, (2001).
- [45] G. Ghigo, G. A. Ummarino, R. Gerbaldo, L. Gozzelino, F. Laviano, and E. Mezzetti, *Phys. Rev. B* **74**, 184518 (2006).
- [46] J. Kortus, O. V. Dolgov, and R. K. Kremer, *Phys. Rev. Lett.* **94**, 027002 (2005).
- [47] S. Agrestini et al., *J. Phys. Condens. Matter* **13**, 11689 (2001).
- [48] J. Y. Xiang et al., *Phys. Rev. B* **65**, 214536 (2002).
- [49] J.Q. Li, L. Li, F.M. Liu, C. Dong, J.Y. Ziang, and Z.X. Zhao, *Phys. Rev. B* **65**, 132505 (2002).
- [50] S. Margadonna et al., *Phys. Rev. B* **66**, 014518 (2002).
- [51] G. Papavassiliou et al., *Phys. Rev. B* **66**, 140514(R) (2002).
- [52] A. Bianconi et al., *Phys. Rev. B* **65**, 174515 (2002).
- [53] O. de la Pena, A. Aguayo, and R. de Coss, *Phys. Rev. B* **66**, 012511 (2002).
- [54] P. Postorino et al., *Phys. Rev. B* **65**, 020507(R) (2001).
- [55] D. Di Castro et al., *Europhys. Lett.* **58**, 278 (2002).
- [56] M. Putti et al., *Phys. Rev. B* **68**, 094514 (2003).
- [57] R. A. Ribeiro et al., *Physica (Amsterdam)* **384C**, 227 (2003); **385C**, 16 (2003).
- [58] H. Schmidt et al., *Phys. Rev. B* **68**, 060508(R) (2003).
- [59] Y. Wang et al., *J. Phys. Condens. Matter* **15**, 883 (2003).
- [60] A. A. Baker et al., *J. Phys. D: Appl. Phys.* **52**, 295302 (2019).
- [61] M. Iavarone, R. Di Capua, A. E. Koshelev, W. K. Kwok, F. Chiarella, R. Vaglio, W. N. Kang, E. M. Choi, H. J. Kim, S. I. Lee, A. V. Pogrebnjakov, J. M. Redwing, and X. X. Xi, *Phys. Rev. B* **71**, 214502 (2005).
- [62] X. X. Xi, *Rep. Prog. Phys.* **71**, 116501(26) (2008).
- [63] A. Ghosal, M. Randeria, and N. Trivedi, *Phys. Rev. Lett.* **81**, 3940 (1998).
- [64] A. Ghosal, M. Randeria, and N. Trivedi, *Phys. Rev. B* **65**, 014501 (2001).
- [65] S. M. Ramos et al., *Phys. Rev. Lett.* **105**, 126401 (2010).
- [66] H. Sakakibara, K. Suzuki, H. Usui, K. Kuroki, R. Arita, D. Scalapino and H. Aoki, *Phys. Rev. B* **86**, 134520 (2012).
- [67] L. Deng, Y. Zheng, Z. Wu, S. Huyan, H. Wu, Y. Nie, K. Cho and C. Chu, *Proc. Natl. Acad. Sci. USA* **116**, 2004 (2019).
- [68] A. M. Black-Schaffer and A. V. Balatsky, *Phys. Rev. B* **88**, 104514 (2013).
- [69] H. Caldas, F. S. Batista, M. A. Continentino, F. Deus, and D. Nozadze, *Ann. Phys.* **384**, 211 (2017).
- [70] G. N. Bremm, M. A. Continentino, and T. Micklitz, *Phys. Rev. B* **104**, 094514 (2021).
- [71] A. Y. Kitaev, *Sov. Phys. Usp.* **44**, 131 (2001).

- [72] R. Wakatsuki, M. Ezawa, Y. Tanaka, and N. Nagaosa, *Phys. Rev. B* **90**, 014505 (2014).
- [73] M. A. Continentino, H. Caldas, D. Nozadze, and N. Trivedi, *Phys. Lett. A* **378**, 3340 (2014).
- [74] M. A. R. Griffith, E. Mamani, L. Nunes, and H. Caldas, *Phys. Rev. B* **101**, 184514 (2020).
- [75] M. Foglio, L. Falicov, *Phys. Rev. B* **20**, 4554 (1979).
- [76] A. A. Aligia, E. Gagliano, L. Arrachea, and K. Hallberg, *Eur. Phys. J. B* **5**, 371 (1998).
- [77] N. N. Bogoljubov II *Nuovo Cimento* (1955-1965) volume **7**, 794 (1958); J. G. Valatin II *Nuovo Cimento* (1955-1965) volume **7**, 843 (1958).
- [78] J.-PetriMartikainen, J. Larson, *Phys. Rev. A* **86**, 023611 (2012).
- [79] S. Yin, J. E. Baarsma, M. O. J. Heikkinen, J.-P. Martikainen, P. Torma, *Phys. Rev. A* **86**, 053616 (2015).
- [80] M. R. Eskildsen et al., *Phys. Rev. Lett.* **89**, 187003 (2002).
- [81] N. Nakai, M. Ichioka, and K. Machida, *J. Phys. Soc. Jpn.* **71**, 23 (2002).
- [82] H. Caldas, A. Celes, D. Nozadze, *Ann. Phys.* **394**, 17 (2018).
- [83] V. Dobrosavljević and G. Kotliar, *Phys. Rev. B* **50**, 1430 (1994).
- [84] T. A. Costi, A. Liebsch, *Phys. Rev. Lett.* **99**, 236404 (2007).
- [85] M. A. Continentino, I. T. Padilha, and H. Caldas, *J. Stat. Mech. Theory Exp.* **2014**, P07015 (2014).
- [86] J. P. Vyasanakere, V. B. Shenoy, *Phys. Rev. B* **83**, 094515 (2011).
- [87] H. Hu, L. Jiang, X.-J. Liu, and H. Pu, *Phys. Rev. Lett.* **107**, 195304 (2011).
- [88] V. Janis, M. Ulmke and D. Vollhardt, *Europhys. Lett.*, **24**, 287 (1993).
- [89] A. Georges, G. Kotliar and W. Krauth, *Z. Phys. B* **92**, 313 (1993).
- [90] R. M. Fernandes, J. T. Haraldsen, P. Wölfle, and A. V. Balatsky, *Phys. Rev. B* **87**, 014510 (2013).
- [91] L. Andersen, A. Ramires, Z. Wang, T. Lorenz, and Y. Ando, *Sci. Adv.* **6**, eaay6502 (2020).
- [92] V. B. Eltsov, T. Kamppinen, J. Rysti, and G. E. Volovik, arXiv:1908.01645.
- [93] Y. Dubi, Y. Meir, Y. and Y. Avishai, *Nature* **449**, 876-880 (2007).
- [94] D. B. Haviland, Y. Liu, and A. M. Goldman, *Phys. Rev. Lett.* **62**, 2180 (1989); J. M. Valles, R. C. Dynes, and J. P. Garno, *ibid.* **69**, 3567 (1992).
- [95] A. E. White, R. C. Dynes, and J. P. Garno, *Phys. Rev. B* **33**, 3549 (1986).
- [96] H. M. Jaeger, D. B. Haviland, A. M. Goldman, and B. G. Orr, *Phys. Rev. B* **34**, 4920 (1986).
- [97] D. Shahar and Z. Ovadyahu, *Phys. Rev. B* **46**, 10917 (1992).
- [98] J. Kim, V. Chua, G. Fiete et al., *Nature Phys.* **8**, 464 (2012).
- [99] H. Caldas, R. O. Ramos, *Phys. Rev. B* **80** (11), 115428 (2009).